Nigerian Journal of Physics (NJP)
ISSN online: 3027-0936
ISSN print: 1595-0611
DOI: https://doi.org/10.62292/njp.v35i2.2026.490
Volume 35(2), June 2026

Determination of Photon Energy Absorption in Epoxy-Based Metallic Composite Samples

***[1]Oluniyi Samuel Makinde, [1]Olaosebikan Akanni Aremu, [2]Oluyemi Samuel Adejuwon and [3]Olatunde Michael Oni**

[1]Department of Physics, The Polytechnic, Ibadan, Nigeria.
[2]Mechanical Engineering Department, Adeseun Ogundoyin Polytechnic, Eruwa. Oyo State, Nigeria.
[3]Department of Pure and Applied Physics, Ladoke Akintola University of Technology, Ogbomoso, Nigeria.

*Corresponding Author's Email: samuelmakinde566@gmail.com

ABSTRACT

This study investigates the absorption of photon energy and the radiation-shielding efficacy of epoxy-based metallic composites that are reinforced with different weight fractions of bismuth oxide (Bi_2O_3) and barium sulfate ($BaSO_4$). Increasing the loading of Bi_2O_3 from 14.29% to 85.71% resulted in a corresponding increase in composite density, from 2.65 g/cm³ to 5.86 g/cm³. This enhancement in density, along with the higher atomic number of Bi_2O_3 relative to $BaSO_4$, contributed to improved ionizing-radiation absorption. Key attenuation parameters, such as mass attenuation coefficient (μ_m), effective atomic number (Z_{eff}), effective electron density (N_{eff}), and half-value layer (HVL), were assessed over photon energies ranging from 81 to 1332.5 keV. Experimental values closely aligned with theoretical XCOM data, validating significant photoelectric absorption at low energies, where the mass attenuation coefficient increased by up to 98% in high-Z-loaded samples. Composites containing increased Bi_2O_3 fractions exhibited enhanced photon attenuation, decreased half-value layer (HVL), and higher effective atomic number (Z_{eff}) compared to $BaSO_4$-rich samples, indicating the shielding benefits of high-Z fillers. $BaSO_4$ enhanced structural uniformity and mechanical integrity, particularly complementing Bi_2O_3 in low-energy regimes. N_{eff} diminished as photon energy increased, indicating a lower probability of photon–electron interactions at higher energies.

Keywords:
Polymer Composite,
NaI(Tl) Scintillation Detector,
Mass Attenuation Coefficient,
Photon Attenuation,
XCOM,
High-Z fillers.

INTRODUCTION

Epoxy resin composites incorporating heavy-metal particles like bismuth oxide (Bi_2O_3) and barium sulfate ($BaSO_4$) present viable alternatives to conventional lead-based shielding materials, owing to their advantageous properties of density, non-toxicity, and structural versatility (Hedaya *et al*., 2022; Khalil *et al*., 2024). The incorporation of high atomic number (Z) fillers into the polymer matrix markedly increases the likelihood of photon interactions, particularly through the photoelectric effect at low photon energies (Karabul *et al*., 2020).

Traditional methods for characterizing gamma-ray attenuation depend on essential parameters, including the mass attenuation coefficient (μ/ρ), linear attenuation coefficient (μ), and half-value layer (HVL) (Marashdeh *et al*., 2016; Abualroos *et al*., 2022). The parameters are critical for assessing the efficacy of shielding materials across different gamma-ray energy levels. The mass attenuation coefficient, which adjusts attenuation relative to sample density, is significantly influenced by composition and atomic number (Berger & Hubbell, 1987). The effective atomic number (Z_{eff}) and effective electron density (N_{eff}) provide additional characterization of the composite's interaction behavior, derivable from both experimental transmission measurements and theoretical cross-section databases.

Lead is the standard for radiation shielding; however, its toxicity and environmental issues have led to the exploration of safer, more sustainable alternatives (Safari *et al*., 2020). Polymer composites reinforced with Bi_2O_3 and $BaSO_4$ utilize the high atomic number of the fillers while maintaining the lightweight, flexible, and durable characteristics of polymers, rendering them suitable for a wide range of applications (Khalil *et al*., 2024).

Despite increasing research efforts, a limited number of studies have comprehensively characterized photon energy absorption parameters (μm, Z_{eff}, N_{eff}) across a

broad energy spectrum in epoxy-metallic composites. Previous works have measured attenuation coefficients at discrete energies (e.g., 59.54 keV to 1.33 MeV) (Marashdeh *et al*., 2016; Hedaya *et al*., 2022), or used simulation techniques without direct experimental validation (Mahmoud *et al*., 2020).

Consequently, this study focuses on the synthesis, experimental characterization, and computational validation of Bi_2O_3- and $BaSO_4$-reinforced epoxy resin composites. The photon attenuation parameters (μm, Z_{eff}, and N_{eff}) were calculated for photon energies ranging from 81 keV to 1332.5 keV. These findings aim to optimize the absorbing properties of these composites and contribute to the development of effective alternatives in radiation protection field.

MATERIALS AND METHODS

Theory of Photon Absorption in Matter

Depending on the photon energy (E) and the atomic number (Z) of the absorber, three main mechanisms control photon interactions in matter: the photoelectric effect, Compton scattering, and pair production. The photoelectric effect predominates at low photon energies (e.g., ≤ 0.5 MeV), particularly in materials with high Z (Knoll, 2010). Compton scattering becomes more important as energy increases; pair production may also play a role at very high energies (> 1.022 MeV), especially in high-Z composites (Agostinelli *et al*., 2003).

The transmitted intensity I follows the Beer-Lambert law as stated in (Eq. 1) (Mahmoud, 2020) when a gamma-ray beam of intensity I_0 travels through a material of thickness t.

$$I = I_0 \exp(-\mu t) \quad (1)$$

Experimental measurements of the incident and transmitted intensities as well as the composite's thickness are necessary for an accurate calculation of μ.

In Eq. (1), μ (cm^{-1}) is the linear attenuation coefficient, which represents the probability per unit path length that a gamma photon will interact with the material via photoelectric absorption, Compton scattering, or pair production. Accurate determination of μ requires experimental measurements of the incident intensityI_0, the transmitted intensityI, and the sample thickness t, as described by Mahmoud (2020).

The mass attenuation coefficient (μ/ρ) is a universal parameter for comparing various materials because it normalizes μ by density (ρ).

The mass attenuation coefficient, denoted as $\mu_m$or (μ/ρ), is a fundamental radiation interaction parameter that describes the attenuation of gamma photons per unit mass of a material. It is obtained by normalizing the linear attenuation coefficient μ by the material density ρ. This normalization removes the influence of physical density, allowing a direct and universal comparison of the intrinsic gamma-ray shielding capabilities of different materials. The mass attenuation coefficient is defined by Eq. (2):

$$\mu_m = {}^{\mu}/_{\rho}\ gcm^{-2} \quad (2)$$

For mixtures, a weighted sum of the constituents can be used to express the total mass attenuation coefficient (Marashdeh et al., 2016).

$$\frac{\mu}{\rho} = \sum_i w_i \left({}^{\mu}/_{\rho}\right)_i \quad (3)$$

where w_i is the weight fraction and$(\mu/\rho)$is the mass attenuation coefficient of the constituent element i. Theoretical tabulations, like those offered by the XCOM program, are frequently compared with accurate values of(μ/ρ) (Berger *et al*., 2010). The cross-sections for atomic ($\sigma_{t,a}$) and electronic ($\sigma_{t,el}$) interactions are used to calculate the effective atomic number (Z_{eff}), which offers a single-number representation of the atomic interaction properties of the composite.

$$Z_{ef} = \frac{\sigma_{t,a}}{\sigma_{t,el}} \quad (4)$$

Similarly, the electron concentration available for photon interactions is captured by effective electron density (N_{eff}). These energy-dependent parameters are helpful in describing the behavior of composite shielding. A useful indicator of the shielding thickness needed to cut photon intensity by 50% is the half-value layer (HVL).

Composite Synthesis and Sample Preparation

The epoxy-based composites were synthesized by incorporating finely ground bismuth oxide (Bi_2O_3) and barium sulfate ($BaSO_4$) powders into a liquid epoxy resin matrix. Figure 1 (A) depicts the initial state of the components prior to mixing, including liquid epoxy resin and micro-sized Bi_2O_3 and $BaSO_4$ powders. In order to maintain a constant total filler content, the fillers were added in controlled proportions ranging from 14.29 weight percent to 85.71 weight percent Bi_2O_3, while $BaSO_4$ was concurrently adjusted in complementary ratios. In order to methodically assess the impact of high-Z material concentration on radiation attenuation performance, this range was chosen.

Mixing was done by progressively adding the metal oxide powder mixtures to the epoxy resin. After mixing the mixtures thoroughly, the mixture was poured into the casting molds, as indicated in Figure 1C. At this point in the process, the mixtures had been thoroughly mixed. Compression molding was used to ensure that the mixtures were compacted optimally. Additionally, compression molding also made it possible for the mixtures to cure in the casting molds. Figure 1B below indicates the step by step process of the mixtures being mixed.

After the curing process was completed, the hardened samples of the composite material (Figure 1D) were extracted from the molds. The experimental measurement of the density of the synthesized samples was carried out by calculating their mass per unit volume.

It was also compared to the theoretical values calculated based on the mixture rule (Marashdeh *et. al* 2016 & Aldhuhaibat *et. al* 2021), which indicated the increment in the density values for samples containing higher Bi_2O_3.

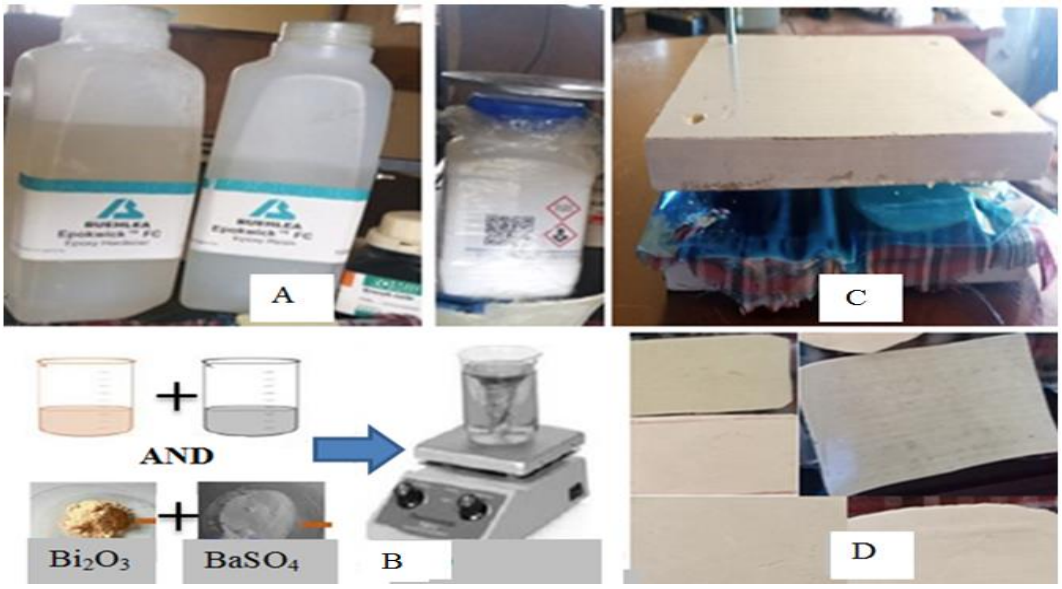

Figure 1: (A) Liquid Epoxy Resin and Micro Powder of Bismuth Oxide and Barium Sulphate. (B) Synthesis of Composite Samples. (C) Cast of Composite Samples. (D) Composite Samples

To provide context for the synthesis process described in the previous section, Table 1 below outlines the composition and density of all the samples synthesized (MP1-MP11). Notably from the table, the increase in the Bi_2O_3 proportion from 14.29 wt % to 85.71 wt % resulted in the increase in the density from 1.65 g/cm³ to 6.86 g/cm³ due to the substantially higher atomic weight and density of Bi_2O_3 compared to $BaSO_4$

Gamma-ray Attenuation Measurements

Gamma-ray attenuation coefficients were measured by means of NaI (Tl) scintillator detectors (dimension: 7.6 × 7.6 cm), accompanied by an analog-to-digital converter and multi-channel analyzer (MCA). Calibration was achieved by standard point sources. These sources included 137Cs (661.7 keV) along with 60Co (1173.2 keV & 1332.5 keV), spanning energies from 59.5 keV to 1332.5 keV (Reeder et al., 2004). Details of energy resolution, count rates, and background levels ensured uncertainty was minimised (Akkurt *et al*., 2014).

Transmission experiments were carried out for each composite sample at various energies. Using the measured values of the incident and transmitted intensities, the values of the linear attenuation coefficients (μ) for the samples were obtained from the Beer-Lambert law. Finally, the values of the mass attenuation coefficients (μ/ρ) for the samples were also obtained.

Table 1: Sample Code Shown Parameters to Optimized (Filler in G and Wt %, Density (P)

Sample code	Filler weight fraction (g)		Filler weight fraction (wt %)		Density(g/cm^3)
	Bi_2O_3	$BaSO_4$	Bi_2O_3	$BaSO_4$	
MP1	10	60	14.29	85.71	1.65
MP2	15	55	21.43	78.57	1.97
MP3	20	50	28.57	71.43	2.29
MP4	25	45	35.71	64.29	2.81
MP5	30	40	42.86	57.14	3.53
MP6	35	35	50.00	50.00	4.26
MP7	40	30	57.14	42.86	4.78
MP8	45	25	64.29	35.71	5.50
MP9	50	20	71.43	28.57	5.92
MP10	55	15	78.57	21.43	6.24
MP11	60	10	85.71	14.29	6.86

Theoretical Calculations of Attenuation Parameters

The theoretical parameters for interaction of the photon (μ/ρ, Z_{eff}, N_{eff}) were calculated from the XCOM photon cross-section data (Berger & Hubbell, 1987). Weight fractions for the elements in the Bi_2O_3, $BaSO_4$, and epoxy components were used to calculate the cross-section values for the interaction processes for the given energies of interest.

RESULTS AND DISCUSSION

Density and Composite Characterization

The increase in the loading level of Bi_2O_3 resulted in an increase in the values of density from 2.65 g/cm³ to 5.86 g/cm³. This observation was consistent with observations made by previous researchers on the effect of the addition of Bi_2O_3 on the epoxy system (Khalil *et al.* 2024). Additionally, the validation of the values of the experimental density against the theoretical values indicated effective dispersion (Limkitjaroenporn *et al.* 2013).

Linear Attenuation Coefficient (LAC)

The linear attenuation coefficient (LAC) increases with higher Bi_2O_3 and $BaSO_4$ filler content, showing improved gamma-ray blocking efficiency in the composites (Figure 2). However, the peak values of the LAC occur in the ranges of 81.0-136.5 keV because of the photoelectric effect. Additionally, the decrease in the values was noted in the range of 276.4-1332.5 keV because of the effect of the Compton scattering (Figure 3). Also from the graphs (MP1-MP11), it was clear that the increment in the bismuth values resulted in the decrease in the transmission values from 1.65% to 15.46% for low energy values. However, for higher energies, the values ranged from 54.45% to 96.60%. Additionally, the attenuation was higher in the 85.71% Bi_2O_3 composite. However, $BaSO_4$ also generated peaks at 56.4 keV and 90.5 keV. Overall, Bi_2O_3 outperforms $BaSO_4$, though both fillers act synergistically to enhance shielding across the measured energy range. The attenuation improvement at higher Bi_2O_3 loadings is comparable to results reported for nano-scale fillers (Tonguc *et al*., 2021).

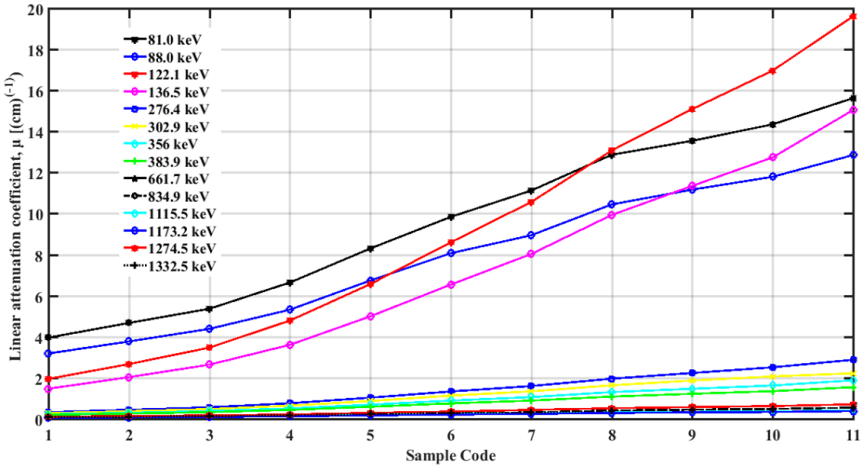

Figure 2: Linear Attenuation Coefficient vs. % Weight of Bismuth and Barium

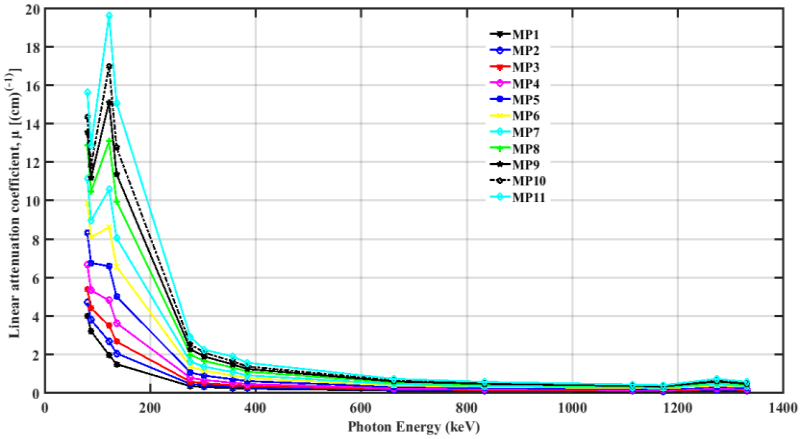

Figure 3: Linear Attenuation Coefficient vs. Photon Energy

Mass Attenuation Coefficient (MAC)

The measured mass attenuation coefficients showed excellent agreement with the theoretical XCOM values. Deviations between the measured values and XCOM results ranged from 0.001 % to 0.012 %. Such good agreement indicates the reliability of the XCOM database in the designing of high-Z composites (Elmahroug & Elbashir, 2015; Prasad & Reddy, 2018). Referring to Figure. 4, for lower photon energies (81–136.5 keV), the MAC showed remarkable escalations reaching 98% for higher proportions of Bi_2O_3. This observation aligns with the prevalence of the photoelectric interaction for lower photon energies (Kumar *et al.,* 2021; Mostafa, 2014). At higher energies beyond 136 keV, the MAC decreased in accordance with the shift to the Compton scattering mechanism, which varies independently of the atomic number (Agostinelli *et al*., 2003).

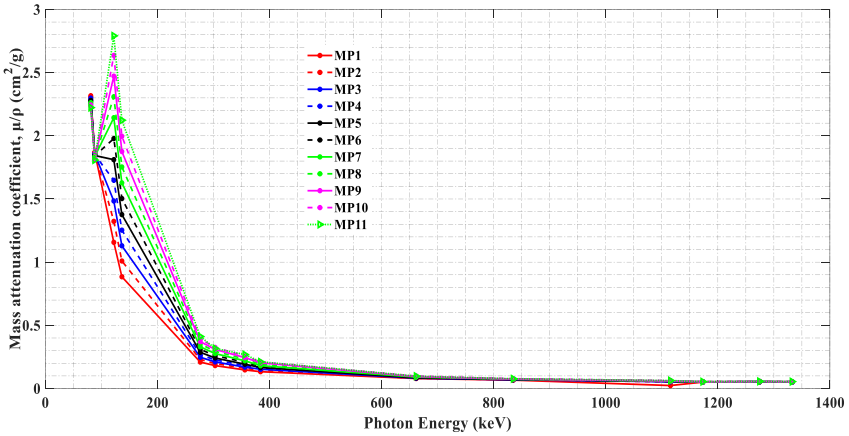

Figure 4: Mass Attenuation Coefficients for Different Percentages of Synthesized Samples For different Energies

Effective Atomic Number (Z_{eff}) and Electron Density (N_{eff})

The effective atomic number (Z_{eff}) rises steeply at lower photon energies, reaching its maximum near 100 keV because of the dominant photoelectric effect mechanism. The observed trend in the present study is consistent with the findings of Rammah *et al*. (2019). Specifically, the parameter decreases sharply up to 2 MeV due to the dominance of the Compton scattering mechanism (Figure 5), followed by a slight increase beyond 1.5 MeV attributed to the onset of pair production.Those composites containing higher proportions of Bi_2O_3 in the mixture, especially MP11/MPP5 (20% Bi_2O_3), contain the maximum Z_{eff} values. However, samples without Bi_2O_3 possess the least values. This clearly proves the Z-dependent nature of the shielding efficiency (Harish 2011; Singh and Badiger 2015). At higher concentrations of $BaSO_4$ in the composites, the values of Z-effect also increase. This is proved by comparing the values in the mixtures MPP1-MPP3 and MPP2-MPP4. At energies beyond 200 MeV, the values of Z_{eff} tend to become constant because the mechanism of interaction becomes less Z-dependent (Harish 2011). Similar variations are noted in the effective electron density (N_{eff}) (Figure 6), reducing sharply at lower energies and rising along with the increase in weight percentage of both Bi and Ba.

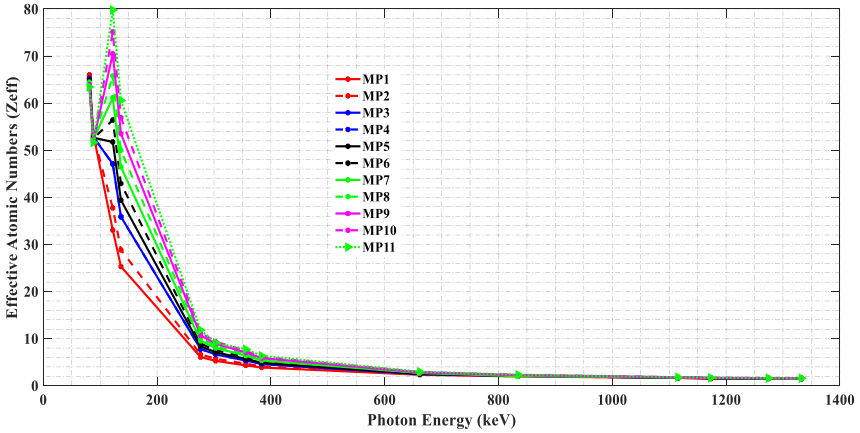

Figure 5: Effective Atomic Number vs. Photon Energy

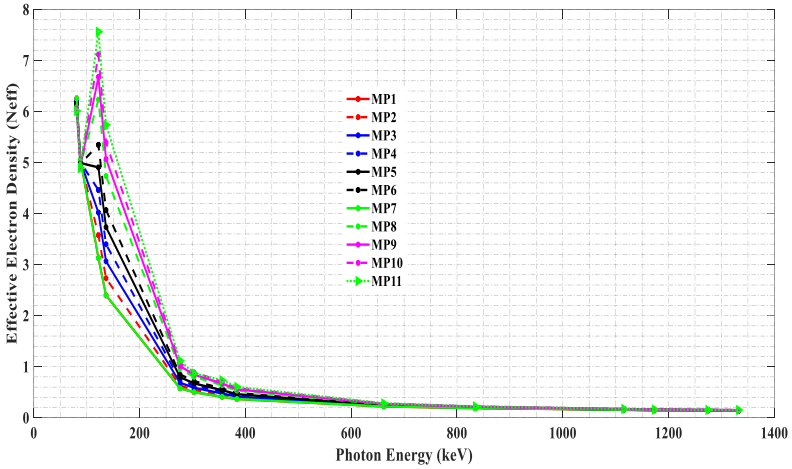

Figure 6: Effective Electron Density vs. Photon Energy

Half-Value Layer (HVL)

The HVL analysis indicates that the Bi_2O_3-based composites provide comparable values to the lead at ~59.5 keV energies, validating their potential for implementation in safe alternatives for radiation protection. However, in the lower ranges of the photon energy scale (e.g. 661.66 keV & 1408.01 keV), the values for the HVL increase for the composites since higher energies correspond to higher penetrating capabilities of the radiation (Aldhuhaibat *et al*., 2021 & Mahmoud *et al*., 2020). Figure 7 plots the same behavior by depicting that the HVL values decrease in the order of composites possessing higher Bi_2O_3 concentrations, viz. the MP 11 (85.71% Bi_2O_3), and further validating the same while the higher the concentrations of the fillers possessing higher atomic numbers (Bi_2O_3 & $BaSO_4$), the lower the values for the HVL. Additionally, the lead continues to maintain its lower values for the HVL measures.

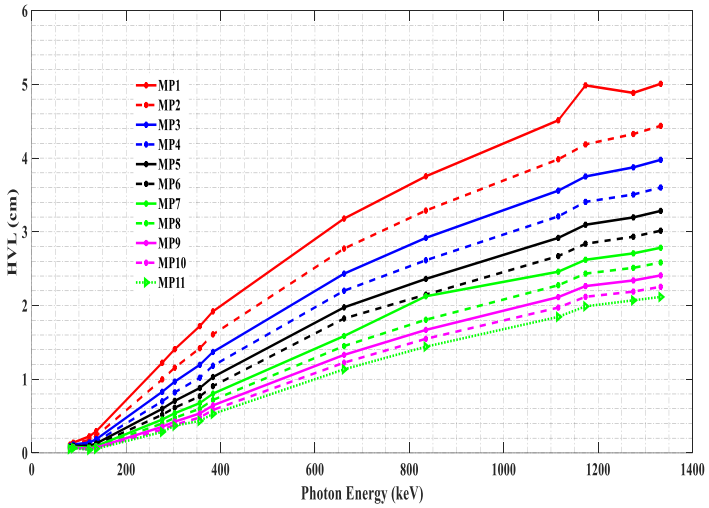

Figure 7: Calculated Half-Value Layer (HVL) vs. Photon Energy

Absorption Efficiency

Absorption efficiency of the developed epoxy-Bi_2O_3-$BaSO_4$ composites clearly indicates the influence of the composition of the fillers used and the energy of the incoming photons. Comparative analysis against metallic absorbers also indicates the authenticity of the absorptivity enhancement in bismuth-based composites (Wang *et al*., 2020). At lower photon energies (81–136.5 keV), composites with higher Bi_2O_3 content exhibited enhanced photon absorption. In particular, MP11 (85.71 wt. % Bi_2O_3) demonstrated superior attenuation performance, achieving attenuation efficiencies exceeding 90%. This improvement is attributed to the increased contribution of the photoelectric effect at low energies. In contrast, $BaSO_4$ increased the detected photon count by introducing sharp spectral peaks at 56.4 keV and 90.5 keV. At higher energies (276.4-1332.5 keV), the Shielding efficiency reduced because of the strong influence of the Compton Effect. Nevertheless, the dense samples having higher atomic numbers continued

to record lower transmission percentage values (3-45%) compared to the lighter ones. These aspects stand clear from Figures 2 and 3. Analysis against the Half Value Layer values (Figure 7) indicates how the Bi_2O_3-dominant composites come very close to the values of pure lead at ~59.5 keV. However, the joint influence of the combination of Bi_2O_3-$BaSO_4$ improves the absorptivity values in the whole measured energy spectrum range.

CONCLUSION

This research indicates that epoxy-based composites reinforced with Bi_2O_3 and $BaSO_4$ present significant potential as viable substitutes for traditional lead radiation absorption. The composites demonstrated increased density (2.65–5.86 g/cm³), enhanced mass attenuation coefficients, elevated effective atomic numbers (Z_{eff}), and improved electron densities (N_{eff}), especially within the low-energy range of 81–136.5 keV, where the photoelectric effect is predominant. The experimental MAC values aligned closely with the XCOM theoretical predictions, thereby validating the accuracy of both the synthesis and measurement processes. High-Bi_2O_3 composites consistently demonstrated superior performance compared to $BaSO_4$-rich samples, although $BaSO_4$ contributed to enhanced mechanical uniformity and additional attenuation peaks. The HVL analysis indicated that the samples with the highest Bi_2O_3 loading exhibited attenuation performance comparable to that of lead at low energy levels. The results collectively validate the synthesized composites as promising, non-toxic, and structurally robust materials for radiation shielding applications. Across a broad photon energy spectrum.

REFERENCES

Abualroos, N. J., Ahmed, M., Alajerami, Y., & Basha, A. (2022). Radiation attenuation effectiveness of polymer-based composites. *Radiation Physics and Chemistry*, *222*, 111070.

Akkurt, İ., Altınsoy, N., Çelik, A., & Mavi, B. (2014). Performance of NaI (Tl) detector for gamma-ray spectroscopy. *Journal of Radiation Research and Applied Sciences*, 7(4), 393–398.

Agostinelli, S., Allison, J., Amako, K., Apostolakis, J., Arce, P., Asai, M., Wright, D. (2003). GEANT4—A simulation toolkit. *Nuclear Instruments and Methods in Physics Research*, 506(3), 250–303.

Aldhuhaibat, M. J. R., Mahdi, K., & Hassan, A. (2021). Improved gamma radiation shielding traits of epoxy composites: Experimental and XCOM comparison. *Radiation Physics and Chemistry* 179, 109183.

Berger, M. J., & Hubbell, J. H. (1987). XCOM: Photon cross sections database. *National Institute of Standards and Technology.*

Hedaya, A., Mahmoud, K., & El-Sayed, A. (2022). Effect of Bi_2O_3 particle size on the radiation-shielding capacity of epoxy composites. *Polymer, 16*(15), 2125. .

Hubbell, J. H., & Seltzer, S. M. (1995). Tables of X-ray mass attenuation coefficients and mass energy-absorption coefficients. NIST.

Karabul, Y., Hassan, H., & Turkmen, I. (2020). Assessment of epoxy-based micro- and nano-Bi_2O_3 and WO_3 composites for radiation shielding. *Radiation Physics and Chemistry*, *26*, 104423.

Khalil, M. M., Hassan, A., & El-Aziz, A. (2024). Impact of nano-Fe_2O_3 on radiation parameters of epoxy composites. *Scientific Reports,* 14, Article 21940.

Mahmoud, K. (2020). Gamma attenuation coefficients of metal-oxide reinforced polymer systems. *Journal of Radiation Research and Applied Sciences*, 13(1), 1–10.

Mahmoud, K. G., El-Sayed, A., & Ramadan, T. (2020). Monte Carlo investigation of gamma radiation shielding for Bi_2O_3–epoxy composites. *Applied Sciences, 13*(3), 1757.

Marashdeh, M., Ababneh, A., & Al-Ajlouni, A. (2016). Determination of the attenuation coefficients of epoxy composites. *Journal of Applied Polymer Science*, 133(12).

Reeder, P. L., Cooper, J., & Ely, J. H. (2004). Performance of large NaI (Tl) gamma-ray detectors (PNNL-14679). *Pacific Northwest National Laboratory*.

Safari, A., Jafari, M., & Rezaei, M. (2020). Development of lead-free materials for radiation shielding: A review. *Journal of Biomedical Physics and Engineering, 14*(3), 229–244.

Elmahroug, Y., & Elbashir, B. (2015). Mass attenuation coefficients and shielding effectiveness of epoxy composites. *Applied Radiation and Isotopes*, 100, 21–28.

Kumar, A., Singh, P., & Kaur, P. (2021). Structural and shielding characterization of Bi_2O_3–epoxy composites. *Journal of Nuclear Materials*, 552, 152–160.

Limkitjaroenporn, P., Kaewkhao, J., & Chewpraditkul, W. (2013). Gamma-ray attenuation properties of metal-doped polymer composites. *Radiation Physics and Chemistry*, 85, 109–115.

Mostafa, A. M. (2014). Optical and gamma-shielding properties of Fe_2O_3 and Bi_2O_3-filled composites. *Journal of Alloys and Compounds*, 617, 625–632.

Prasad, S. G., & Reddy, K. R. (2018). Determination of mass attenuation coefficients in polymeric materials containing high-Z additives. *Radiation Effects and Defects in Solids*, 173(9–10), 760–772.

Rammah, Y. S., Elmahroug, Y., & Sayyed, M. I. (2019). Photon attenuation parameters of various lead-free composites. *Journal of Non-Crystalline Solids*, 509, 80–89.

Sharma, M. K., & Singh, R. (2020). Shielding behavior of bismuth-reinforced polymer composites at photon energies up to 1.33 MeV. *Materials Today Communications*, 25, 101–112.

Singh, V. P., & Badiger, N. M. (2015). Effective atomic numbers for composite materials exposed to gamma radiation. *Nuclear Engineering and Design*, 292, 175–182.

Tochaikul, G., Supakun, P., & Khumkong, P. (2025). Enhancing radiation shielding capabilities using epoxy-resin composites reinforced with coral-derived calcium carbonate. *Polymers,* 17(1), 113.

Tonguc, B., Ozdemir, Y., & Yılmaz, E. (2021). Gamma-ray energy absorption in nano- and micro-scale Bi_2O_3 polymer composites. *Radiation Physics and Chemistry*, 188, 109–117.

Wang, B., Li, Z., Chen, J., & Zhao, Y. (2023). A comparative study between pure bismuth/tungsten and the bismuth tungsten oxide for flexible shielding of gamma/X rays. *Radiation Physics and Chemistry, 208*, 110906.